Barium Tetratitanate MIC Technology

YOUNG SOO LEE, MEMBER, IEEE, WILLIAM J. GETSINGER, SENIOR MEMBER, IEEE, AND LAWRENCE R. SPARROW

Abstract—**Experimental results on $BaTi_4O_9$ microwave integrated circuit (MIC) characteristics, including microstrip dispersion and loss, have shown excellent agreement with the theoretical predictions. Precision measurements of temperature stability were conducted at 14 GHz. The high dielectric constant ($\epsilon_r = 37$) and its negative temperature coefficient can be used in specialized MIC's for application to advanced microwave subsystems.**

I. Introduction

TEMPERATURE-STABLE, low-loss, and high-permittivity dielectric materials have been investigated for application to microwave filters, oscillators, phase control, and other circuits [1]–[3]. Barium oxide–titanate compounds [2],[4]–[6] and a series of zirconate compounds [1],[7] have been developed as candidates for the ultrastable microwave dielectric. Recently, barium nonatitanate ($Ba_2Ti_9O_{20}$) ceramics have been successfully used in temperature-stable microwave dielectric resonator filters [6] with average temperature coefficients of less than $2\times10^{-6}/°C$. These ceramics may replace the conventional bulky expensive heavy Invar waveguide filters in which thermal stability is the major consideration.

The negative dielectric temperature coefficient of barium tetratitanate ($BaTi_4O_9$) and the useful microstrip characteristics have been known [2]. However, $BaTi_4O_9$ microstrip dispersion has not been verified, and $BaTi_4O_9$ microstrip design data for frequencies beyond 11 GHz have not been published.

This paper presents the metallization and fabrication processes of $BaTi_4O_9$ MIC's and the experimental results on $BaTi_4O_9$ microstrip dispersion and transmission loss up to 18 GHz. In addition, transmission phase thermal stability was measured, and the dielectric constant temperature coefficient was determined at 14 GHz.

II. MIC Fabrication Process

The purchased substrates are lapped and polished with a 7-μin rms or better finish (finishes as fine as a 2-μin rms have been achieved.) Cleaning is limited to ultrasonic water and alcohol soaks, followed by flushing with a clean solvent. Since metallization is by sputtering, further cleaning is accomplished by sputter etching, which has been modified to prevent thermal cracking caused by heat buildup. (A temperature rise of $>300°C$ is possible.) Chromium is then sputtered at a nominal 150-Å thickness, followed by 1000 Å of gold.

The metallized substrates are spin coated with a positive photo resist, and the required circuit pattern is exposed in a mask aligner and developed. The substrate is then pattern-pulse plated with gold to the desired circuit thickness (~4 μm), the resist is removed, and the unwanted sputtered gold and chromium chemically etched. Chromium is more difficult to remove completely from $BaTi_4O_9$ than from less active substrate materials, and a final etch in dilute nitric–hydrofluoric acid is required. In this process, circuit tolerances are maintained to ±5 μm or less.

Because of the mechanical characteristics of $BaTi_4O_9$, its handling and processing are more difficult than those of the more familiar alumina and fused silica. $BaTi_4O_9$ is subject to thermal shock cracking. It can be machined using diamond blades and is also more reactive chemically than alumina and silica, thereby limiting the cleaning procedures and requiring greater control of the etching processes. Physical properties of the material are given in [2].

III. Microstrip Circuit Characteristics

The $BaTi_4O_9$ microstrip dispersion and transmission loss characteristics have been evaluated experimentally up to 18 GHz. Initially, $BaTi_4O_9$ substrates ($0.015\times2.0\times2.0$ in) were procured from Trans-Tech and Ampex. The surface finish of the substrates was 2-μin rms for the test MIC's.

A. $BaTi_4O_9$ Microstrip Dispersion

Previous measurements [2] of $BaTi_4O_9$ in a radial cavity revealed no dielectric relaxation through 11 GHz. Present data on the microstrip dispersion [8] measurements using very loosely coupled transmission resonators (Fig. 1(a)) show a nondispersive material characteristic in $BaTi_4O_9$ up to at least 18 GHz. A precision-measurement technique for microstrip dispersion and the results are described herein.

Fig. 1(a) shows the very loosely coupled transmission-line resonator model. The resonator electrical length L_e, is determined by $L_e = L_p + 2\Delta$, where L_p is the physical length and Δ is the equivalent line length due to the open-end foreshortening effect [10],[11]. The end coupling gap g, has a high transmission loss, typically 45–55 dB, at

Manuscript received October 16, 1978; revised March 6, 1979. This paper was based upon the work performed at COMSAT Laboratories under the sponsorship of Communications Satellite Corporation.

The authors are with COMSAT Laboratories, Clarksburg, MD 20734.

0018-9480/79/0700-0655$00.75 ©1979 IEEE

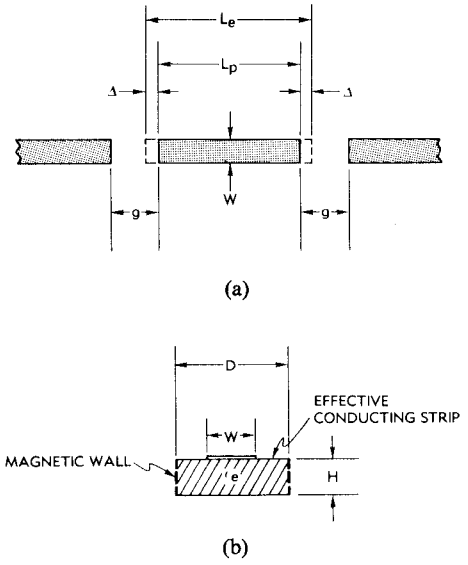

Fig. 1. (a) Microstrip transmission resonator. (b) Parallel-plate model of microstrip.

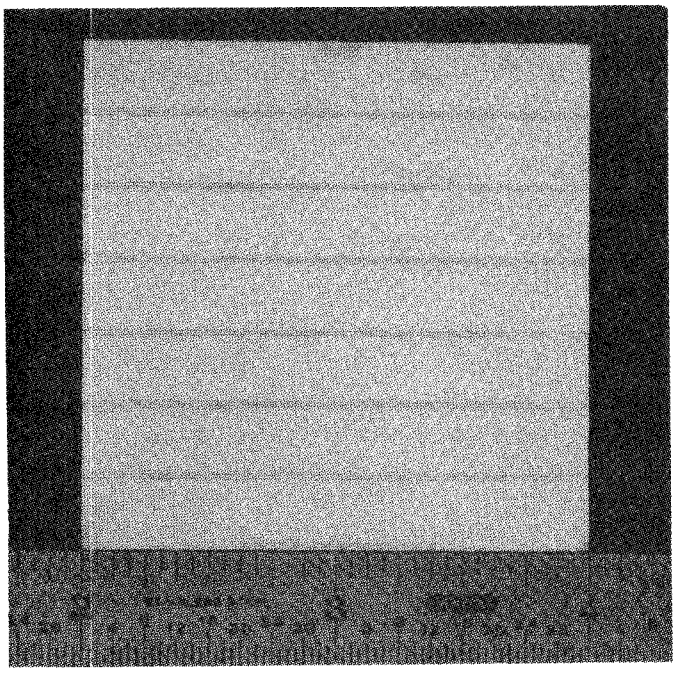

Fig. 2. Transmission resonators for microstrip dispersion measurements.

resonance frequencies. This condition is considered sufficient to omit any series coupling-capacitance effect in the gap g, for the Δ correction term.

Fig. 2 shows photographs of the transmission-line resonators used for the $BaTi_4O_9$ microstrip dispersion measurements, with fundamental resonance frequencies ranging from 1 to 9 GHz. The substrate is 0.015 in thick, and the substrate relative dielectric constant was measured at 1 MHz with a Boonton capacitance bridge on 0.5×0.5-in metallized substrates. The capacitance measurements of the $BaTi_4O_9$ substrates indicated that the relative dielectric constant ϵ_r, is 37.0 with ±2-percent tolerance. The resonator strip width (W) to substrate

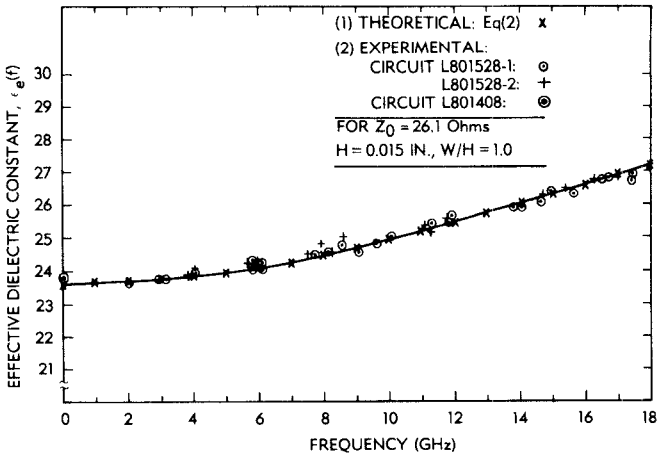

Fig. 3. $BaTi_4O_9$ microstrip dispersion.

thickness (H) ratio is 1, and the characteristic impedance (Z_o) is 26.1 Ω. The end coupling gap g is typically 0.022 in for the resonators.

Transmission resonant frequencies were measured using an automatic network analyzer, and the effective dielectric constant was computed by

$$\epsilon_e(f)=\left[\frac{cn}{2f_n(L_p+2\Delta)}\right]^2 \tag{1}$$

where c is the velocity of light in vacuum (11.803×10^9 in/s), f_n is the resonant frequency of order n (i.e., $n=1,2,\cdots,N$) times the fundamental resonant frequency determined by the effective length $L_p+2\Delta$. The length increment Δ, essentially frequency independent, was derived theoretically from [10]; $\Delta/H=0.31$ (i.e., $\Delta=0.00465$ in) was used for the resonators described above.

The measured effective dielectric constant versus frequency is shown in Fig. 3. All the data points fit within a 2-percent circuit tolerance limit to the LSE model theoretical dispersion equation [8]:

$$\epsilon_e(f)=\epsilon_r-\frac{\epsilon_r-\epsilon_e(0)}{1+G(f/f_p)^2} \tag{2}$$

where $f_p=Z_o/2\mu_0 H$, $\mu_0=31.9186$ nH/in, and G is an empirical factor. An improved G-factor [12] for calculating dispersion by (2) was used:

$$G=\frac{\pi^2}{12}\frac{\epsilon_r-1}{\epsilon_e(0)}\sqrt{\frac{2\pi Z_o}{\eta_0}} \tag{3}$$

where $\eta_0=376.6$ Ω.

The microstrip effective dielectric constant at zero frequency $\epsilon_e(0)$, was computed using the MSTRIP program [13]. Capacitance measured at 1 MHz on a long microstripline (Fig. 4) was used for the characterization of $\epsilon_e(0)$. Assuming a TEM line,

$$\epsilon_e(0)=(cCZ_o)^2 \tag{4}$$

where C is measured in farads per-unit-length (see Fig. 1(b)).

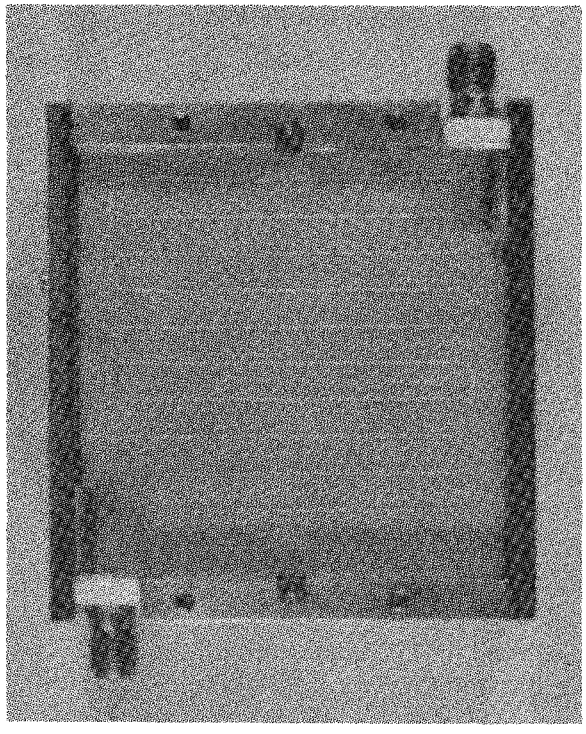

Fig. 4. Meandered $BaTi_4O_9$ microstripline.

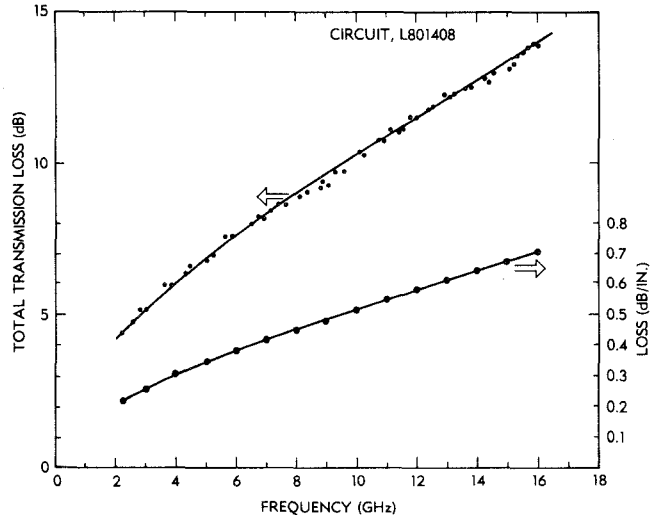

Fig. 5. Experimental transmission loss in $BaTi_4O_9$ microstripline —(19.887-in 26.1-Ω line, $H = 0.015$ in).

Measurements on the 20-in microstripline of Fig. 4 showed $\epsilon_e(1\text{ MHz}) = 23.9$, using (4). The MSTRIP computed value was $\epsilon_e(0) = 23.6$. This demonstrates agreement between the theoretical and experimental values of the near-zero-frequency effective dielectric constant in a $BaTi_4O_9$ microstrip, and indicates an isotropic characteristic for the substrate.

B. Losses In Microstrip

Microstrip loss for a nonmagnetic dielectric substrate is the sum of conductor, dielectric, and radiation losses. The 20-in meandered 26-Ω microstripline in Fig. 4 was used to measure the transmission-line loss constant. The use of the long line without significant discontinuities avoids

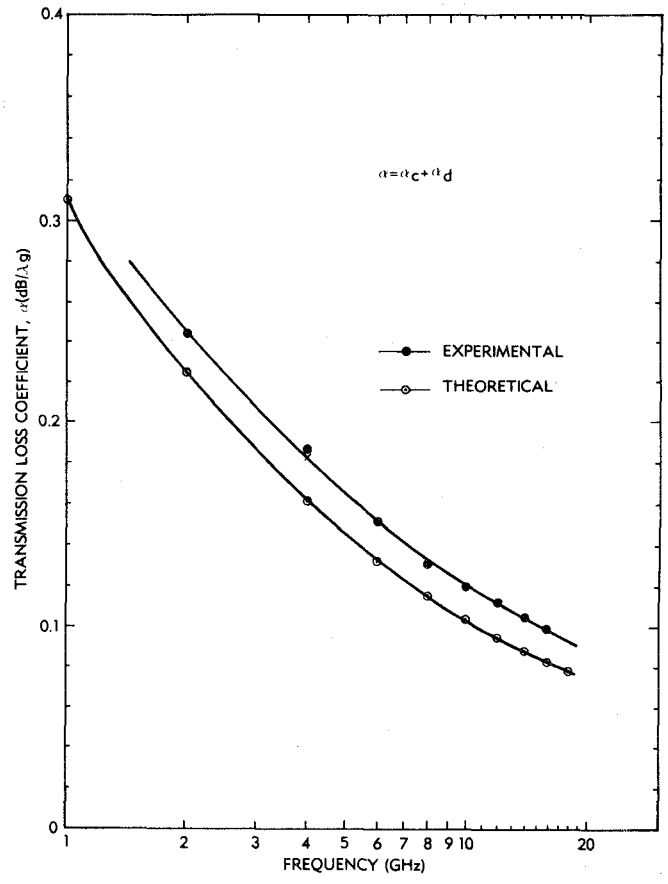

Fig. 6. Theoretical and experimental transmission loss coefficient of 26-Ω $BaTi_4O_9$ microstripline.

radiation occurring in loss measurements using resonators [14]. The wave launcher transitions included $\lambda/4$ impedance transformer sections, and the input return losses were > 12 dB. The circular bend discontinuity effects on the folded line were measured in the swept frequency response. An equivalent circuit analysis using an approximate lumped circuit model for the circular bends of the meandered microstripline agreed reasonably well with the swept frequency transmission/reflection measurements when the spacing S, between adjacent lines was large, $S \geqslant 10H$.

Fig. 5 shows the actual measured transmission loss versus frequency for the 19.887-in-long 26-Ω microstripline (on 0.015-in-thick $BaTi_4O_9$ substrate). Fig. 6 shows the normalized transmission loss coefficient (from Fig. 5) in dB/λ_g where the computation of λ_g included the microstrip-dispersion data of Fig. 3. The theoretical transmission coefficient in Fig. 6 was computed as the sum of the conductor loss α_c, and dielectric loss α_d. Microstrip-conductor loss has been formulated using the "incremental inductance rule" by Pucel *et al.* [15]. For $1/2\pi < W/H < 2$, it was shown that

$$\frac{\alpha_c Z_o H}{R_s} = \frac{8.686}{2\pi}\left[1-\left(\frac{W'}{4H}\right)^2\right] \cdot\left[1+\frac{H}{W'}+\frac{H}{\pi W'}\left(\ln\frac{2H}{t}-\frac{t}{H}\right)\right] \quad (5)$$

where

$R_s = (\pi f \mu \rho)^{1/2}$;
$W' = W + \Delta W$;
$\Delta W = t/\pi(\ln 2H/t + 1)$, for $W/H \geqslant 1/2\pi$ and t = conductor thickness.

For the microstripline in Fig. 4 ($W/H = 1.0$, $H = 0.015$ in, $t = 0.00012$ in, $Z_o = 26.1\ \Omega$), (5) yields

$$\alpha_c = \frac{4.863\ R_s}{Z_o H}\ \text{dB/unit length.} \tag{6}$$

The surface resistivity of the gold conducting strip is $R_s = 9.487 \times 10^{-3} \times \sqrt{f(\text{GHz})}$. With the addition of a loss increase of about +3 percent due to a substrate surface roughness [16] of 3-μin rms, the actual surface resistivity becomes

$$R_s = 9.772 \times 10^{-3} \sqrt{f(\text{GHz})}\ . \tag{7}$$

The effect of about a 100-Å layer of chromium adhesive material is negligible in R_s [16]. The conductor-loss coefficient computed by (6) is 77-percent lower than that derived assuming uniform current distribution on the conducting strip, which is valid only for very wide strips, $W/H > 2$.

The conductor-loss coefficient for the test microstripline is

$$\alpha_c = 1.4392\left[\epsilon_e(f) f(\text{GHz})\right]^{-1/z}\ \text{dB/wavelength.} \tag{8}$$

The microstrip dielectric loss constant is obtained from

$$\alpha_d = \frac{8.686\pi}{Q_d}\ \text{dB/wavelength} \tag{9}$$

where Q_d is the quality factor defined by the dielectric loss tangent

$$Q_d \simeq \frac{1}{\tan\delta}\left(1 + \frac{1-q}{q\epsilon_r}\right) \tag{10}$$

where q is the filling factor defined by $q = [\epsilon_e(f) - 1]/(\epsilon_r - 1)$. Equation (10) shows that Q_d is weakly frequency dependent, and can be considered a constant. The loss tangent of $BaTi_4O_9$ is specified as $\tan\delta \leqslant 0.0005$ (at 6 GHz) by the manufacturer. Thus the dielectric loss coefficient is given by

$$\alpha_d = 0.0134\ \text{dB/guide wavelength} \tag{11}$$

for the $BaTi_4O_9$ substrate.

The overall transmission loss coefficient is $\alpha = \alpha_c + \alpha_d$, which is depicted as a theoretical curve in Fig. 6. Fig. 6 shows that the experimental loss coefficient demonstrates good agreement with the theoretical exception of a constant 0.016 dB/wavelength addition from 2 to 18 GHz. The additional constant loss portion may be attributed to connector discontinuity transition losses, as well as a possibly higher loss tangent value tolerance than quoted by the substrate manufacturer.

IV. Thermal Stability Measurements

The transmission phase ϕ, in a transmission line is written as a function of frequency and temperature T, as follows:

$$\phi = -(2\pi/c) f \sqrt{\epsilon_e(f,T)}\ l(T) \tag{12}$$

where $\epsilon_e(f,T)$ is an effective dielectric constant, and $l(T)$ is the length of the transmission line. Equation (2) can be manipulated to show that effective dielectric constant is a nearly linear function of substrate dielectric constant. Thus over-moderate ranges of frequency and temperature

$$\epsilon_e(f,T) = A(f)\epsilon_r(T) + B(f). \tag{13}$$

If a differential expression $d\phi/dT$ of (12) around $T = T_o$ at a fixed frequency is assumed, it is shown that

$$\frac{1}{\phi_o}\frac{\Delta\phi}{\Delta T} = -\left(\frac{1}{l_o}\frac{\Delta l}{\Delta T} + \frac{1}{2}\frac{1}{\epsilon_{eo}}\frac{\Delta\epsilon_e}{\Delta T}\right) \tag{14}$$

where $\phi_o = (2\pi/c) f l_o \sqrt{\epsilon_{eo}}$, and subscript o represents the parameters at $T = T_o$. In a high-dielectric microstripline, $A\epsilon_r \gg B$, therefore,

$$\frac{1}{\epsilon_{eo}}\frac{\Delta\epsilon_e}{\Delta T} = \frac{1}{A\epsilon_r + B}\frac{A\Delta\epsilon_r}{\Delta T} \simeq \frac{1}{\epsilon_r}\frac{\Delta\epsilon_r}{\Delta T}. \tag{15}$$

With a substitution of (15) into (14), the dielectric temperature coefficient is given by

$$\frac{1}{\epsilon_r}\frac{\Delta\epsilon_r}{\Delta T} \simeq -2\left(\frac{1}{l_o}\frac{\Delta l}{\Delta T} + \frac{1}{\phi_o}\frac{\Delta\phi}{\Delta T}\right). \tag{16}$$

Equation (16) indicates that the substrate dielectric temperature coefficient can be determined from measurements of the transmission phase temperature coefficient of the MIC line and the linear thermal-expansion coefficient of the substrate.

A precision-measurement technique of the transmission phase temperature coefficient [17], the modified "Pi-point method," was used to characterize the phase thermal stability of the 20-in $BaTi_4O_9$ microstripline in Fig. 4. The inset of Fig. 7 shows the test circuit configuration. The MIC line was very loosely coupled to the external circuit by the series capacitances C_c, which were obtained as the air gap capacitances between the connector center conductors and the conducting strip.

The transmission resonance peak frequencies were measured at different temperatures. The transmission amplitude versus frequency response of the test circuit is shown in Fig. 7 for a temperature range of −5 to +55°C. The average transmission-phase coefficient is determined by

$$\frac{1}{\phi_o}\frac{\Delta\phi}{\Delta T} = \frac{1}{N}\sum_{i=1}^{N}\frac{1}{f_{oi}}\frac{\Delta f_i}{\Delta T} \tag{17}$$

where i represents the ith transmission peak within the measuring frequency band, f_{oi} is the ith peak frequency at

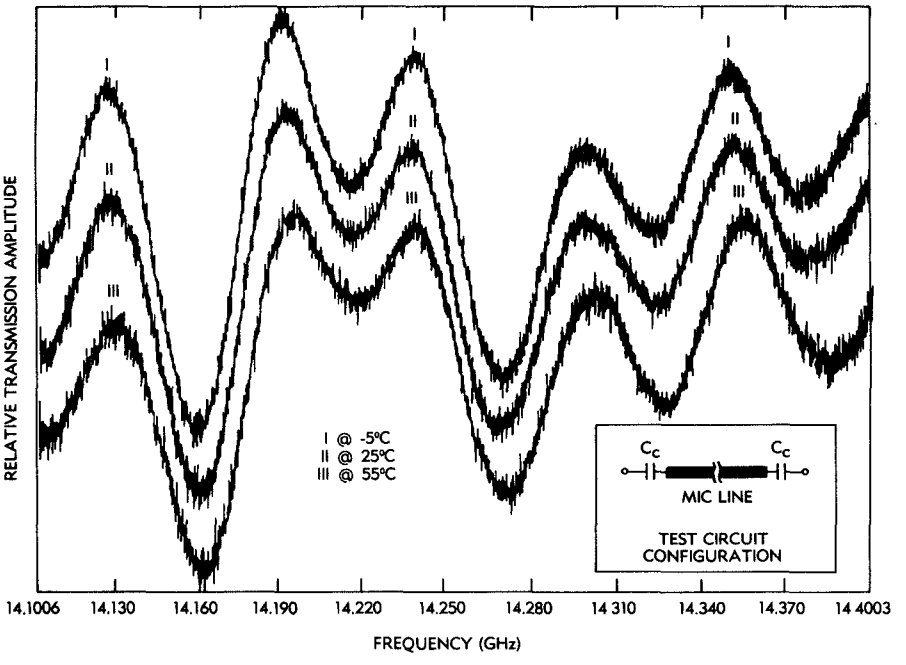

Fig. 7. Temperature stability measurements on $BaTi_4O_9$ MIC line.

TABLE I
THERMAL CHARACTERISTICS OF DIELECTRICS

Material	Relative Dielectric Constant (ϵ_r) at 25°C	Fractional Temperature Coef. of ϵ_r (ppm/°C)	Linear Thermal Expansion Coefficient (ppm/°C)	Thermal Conductivity at 23°C (cgs units)	Remarks
Fused Silica	3.85	+13			GE
	3.82	+25	0.5	0.0033	Dynasil at 8.6 GHz
	3.78	+12			Corning at 14 GHz
Alumina	9.8	+136	6.6	0.070	3M-Co at 10 GHz
Sapphire					
//C-axis	11.53	+141	6.7	0.10	Adolf Meller Co.
⊥C-axis	9.35	+110	5.0	--	at 9 GHz
Beryllia	6.8	+107	7.5	0.620	3M-Co at 10 GHz
$BaTi_4O_9$	37	-26.5	9.4	0.005	Trans. Tech at
	38	-50			14 GHz [1]
Others [1]					
$BaZrO_3$	40	-300			
TiO_2	90	-800			
$CaTiO_3$	150	-1850			
$SrTiO_3$	200	-3000			
$MgTiO_3$	16	+100			
$CaZrO_3$	30	+40			
$SrZrO_3$	38	+120			
$CaTiSiO_5$	45	+1200			

$T = T_o$ (typically at room temperature), and Δf_i is the ith peak frequency shift with a temperature change of ΔT.

From Fig. 7, the average transmission-phase temperature coefficient in the $BaTi_4O_9$ microstripline was determined to be 3.88×10^{-6} part/°C at about 14.25 GHz within -5 to $+55$°C. The linear thermal-expansion coefficient of $BaTi_4O_9$ is 9.4 ppm/°C. Therefore, the dielectric temperature coefficient of $BaTi_4O_9$ is determined using (16) to be -26.6 ppm/°C.

Table I lists the thermal characteristics of typical microwave dielectrics. The expected MIC temperature stability using these substrates can be computed using (14). According to the test results at $T = 25° \pm 30$°C, $BaTi_4O_9$ provides the most thermally stable MIC medium among

the listed dielectric materials, and the $Ba_2Ti_9O_{20}$ substrate (which was not available for evaluation) may provide an even better thermal stability.

V. Conclusions

The experimental evaluation of $BaTi_4O_9$ substrates (supplied by Trans-Tech, Inc.) showed well-controlled dielectric properties, e.g., $\epsilon_r = 37$ (± 2 percent) and isotropic without any material dispersion up to 18 GHz. The microstrip dispersion and loss measurements showed excellent agreement with theoretical results. The dielectric temperature coefficient was -26.6 ppm/°C at 14.25 GHz within the temperature range of -5 to $+55$°C. The 14-GHz microstripline showed transmission-phase temperature stability of $+3.88$ ppm/°C. The negative dielectric temperature coefficient can be used for temperature stable component designs up to 18 GHz. Temperature compensation can be obtained using ordinary positive dielectric temperature coefficient MIC sections, such as sapphire and quartz.

Acknowledgment

The authors wish to acknowledge the efforts of W. Chang, E. Bainbridge, and R. Barber for the barium tetratitanate MIC fabrication processes.

References

[1] R. C. Kell *et al.*, "High-permittivity temperature stable ceramic dielectrics with low microwave losses," *J. Amer. Ceram. Soc.*, vol. 56, no. 7, pp. 352–354, July 1973.

[2] D. J. Masse *et al.*, "A new low-loss high-K temperature-compensated dielectric for microwave applications," *Proc. IEEE*, pp. 1628–1629, Nov. 1971.

[3] J. K. Plourde, "Frequency stability of dielectric resonator oscillators," 1978 IEEE MTT-S *Int. Microwave Symp. Dig.*, p. 480.

[4] H. M. O'Bryan, Jr., J. Thomson, Jr., and J. K. Plourde, "A new BaO-TiO_2 compound with temperature-stable high permittivity and low microwave loss," *J. Amer. Ceram. Soc.*, vol. 57, no. 10, pp. 450–453, Oct. 1974.

[5] J. K. Plourde *et al.*, "$Ba_2Ti_9O_{20}$ as a microwave dielectric resonator," *J. Amer. Ceram. Soc.*, vol. 58, no. 9–10, pp. 418–420, Sept.–Oct. 1975.

[6] J. K. Plourde and D. F. Linn, "Microwave dielectric resonator filters utilizing $Ba_2Ti_9O_{20}$ ceramics," 1977 IEEE MTT-S *Int. Microwave Symp. Dig.*, pp. 290–293.

[7] E. R. Batliwala and C. S. Aitchison, "A low temperature dependent microstrip substrate," *Proc. IEEE*, vol. 65, pp. 1207–1208, Aug. 1977.

[8] W. J. Getsinger, "Microstrip Dispersion Model," *IEEE Trans. Microwave Theory Tech.*, vol. MTT-21, pp. 34–39, Jan. 1973.

[9] ——, "Dispersion of parallel-coupled microstrip," *IEEE Trans. Microwave Theory Tech.*, vol. MTT-21, pp. 144–145, Mar. 1973.

[10] D. S. James and S. H. Tse, "Microstrip end Effects," *Electron. Lett.*, vol. 8, no. 2, pp. 46–47, Jan. 27 1972.

[11] P. Silvester and P. Benedek, "Equivalent capacitances of microstrip open circuits," *IEEE Trans. Microwave Theory Tech.*, vol. MTT-20, pp. 511–515, Aug. 1972.

[12] O. Jensen and E. O. Hammerstad, private communication, ELAB, Norway, Mar. 1977.

[13] T. G. Bryant and J. A. Weiss, "MSTRIP (parameters of microstrip)," *IEEE Trans. Microwave Theory Tech.*, vol. MTT-19, pp. 418–419, Apr. 1971.

[14] E. Belohoubek and E. Delinger, "Loss considerations for microstrip resonators," *IEEE Trans. Microwave Theory Tech.*, vol. MTT-23, pp. 522–526, June 1975.

[15] R. A. Pucel, D. J. Masse, and C. P. Hartwig, "Losses in microstrip," *IEEE Trans. Microwave Theory Tech.*, vol. MTT-16, pp. 342–350, June 1968. "Correction to 'Losses in microstrip'," vol. MTT-16, p. 1064, Dec. 1968.

[16] H. Sobol and M. Caulton, "Technology in Microwave Integrated Circuits," *Advances in Microwaves*, vol. 8, New York: Academic, 1974.

[17] Y. S. Lee, "14-GHz MIC 16-ns Delay Filter for differentially coherent QPSK regenerative repeater," 1978 IEEE MTT-S *Int. Microwave Symp. Dig.*, pp. 37–40.